Mohammad Islam
Department of Computer Science
and Electrical Engineering,
University of Maryland Baltimore County,
Baltimore, MD 21250

Douglas Janssen
Department of Computer Science
and Electrical Engineering,
University of Maryland Baltimore County,
Baltimore, MD 21250

Carlos Romero-Talamas
Department of Mechanical Engineering,
University of Maryland Baltimore County,
Baltimore, MD 21250

Dan Kostov
Department of Cell Biology & Molecular Genetics,
University of Maryland Baltimore County,
Baltimore, MD 21250

Wanpeng Wang
Department of Mechanical Engineering,
University of Maryland,
College Park, MD 20742

Zhongchi Liu
Department of Cell Biology & Molecular Genetics,
University of Maryland,
College Park, MD 20742

Narsingh B. Singh
Department of Chemistry and Biochemistry,
University of Maryland Baltimore County,
Baltimore, MD 21250

Fow-Sen Choa
Department of Computer Science
and Electrical Engineering,
University of Maryland Baltimore County,
Baltimore, MD 21250

Nuclear Radiation Monitoring Using Plants

Plants exhibit complex responses to change in environmental conditions such as radiant heat flux, water quality, airborne pollutants, and soil contents. We seek to utilize natural chemical and electrophysiological response of plants to develop novel plant-based sensor networks. Our present work focuses on plant responses to nuclear radiation—with the goal of monitoring plant responses as benchmarks for detection and dosimetry. In our study, we used plants including Cactus, Arabidopsis, Dwarf mango (pine), Euymus, and Azela. We demonstrated that these plants Chlorophyll-a (F_{680}) to Chlorophyll-b (F_{735}) ratio can be changed according to the radiation dose amount. The recovery processes and speed are different for different plants. [DOI: 10.1115/1.4040364]

Keywords: nuclear monitoring, nuclear detections, Chlorophyll fluorescence, plant electricity

Introduction

Recently, we demonstrated that nearly all plants produce electricity and act as electrical power sources [1,2]. We also found that nuclear radiation alters plant electricity and produces voltage and current changes, which can be used for nuclear detections [1,2]. We further found that nuclear radiation can change plant optical characteristics and cell mechanical structure, which can be associated with macroscopically measurable quantities. This led to the idea that one can explore the history of nuclear activities in an area by examining the recorded information from local plants through a two-tier approach: First, a quick survey through simple electricity response, optical absorption or fluorescence, mechanical strength, etc. measurements to identify possible nuclear activity records and second, a detailed examination through molecular biology techniques to verify both short-term and long-term nuclear activities with low false alarm.

The physical condition and health of plant vegetation as a whole can be monitored by optical spectroscopic methods. Several optical methods can be applied to characterize the leaves and plants by specific spectral signatures. These are absorption spectra, reflectance spectra, and fluorescence spectra as well as photo acoustic spectra [2–5].

Experimental Setup for Radiation Beam and Measuring Fluorescence

The plant radiation studies were done with a neutron beam facility located at the National Institute of Standards and Technology (NIST) Center for Neutron Research (NCNR) Beam Tube 2 (BT-2). The NCNR BT-2 provides an intense source of thermal neutrons that is collimated using a tapered plug (1 and 2 in Fig. 1). This conically shaped beam is nearly uniform in intensity across the area of the beam at image planes downstream. This type of optical arrangement is generally referred to as pinhole optics.

Although the CNR produces mostly thermal neutrons, there are still a significant amount of high energy neutrons (HEN) and gamma rays as a byproduct. These HEN and gamma rays represent a background that can be dangerous to electronic equipment. Therefore, a HEN and gamma ray filter is placed directly downstream of the tapered collimator. This filter consists of 10 cm of

Manuscript received August 23, 2017; final manuscript received March 16, 2018; published online September 10, 2018. Assoc. Editor: Michal Kostal.

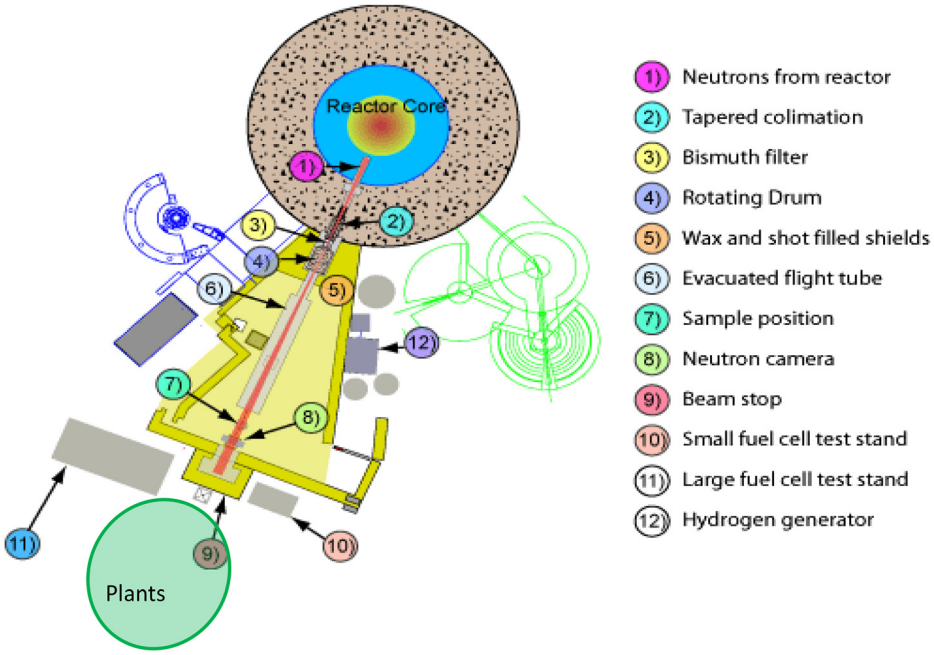

Fig. 1 Plan view of the neutron imaging facility pointing out some major features

bismuth single crystal cooled to liquid nitrogen temperatures (−196.1 °C). Cooling the bismuth dramatically reduces the vibrational phonon modes in the crystal, which strongly scatter thermal neutrons. The cooled crystal becomes nearly transparent (60% transmission) to thermal neutrons and strongly filters the HEN by diffraction and gamma rays by absorption coming from the reactor core.

Two exposure tests were conducted in 2014. One was in July and the other was in September. Each lasted about 3 days long. We used ocean optics dragon spectrometer. Ocean optics dragon spectrometer is a 2048-element linear silicon charge-coupled device array detector. It is responsive from 350 to 900 nm. It has an optical resolution of ∼2.0 nm full width at half maximum with a 50 μm (radius) fiber, and integration time from 3 ms to 65 s.

Sample tree subjects were placed at a distance of ∼3 m from NIST BT-2 reactor gate capable of producing a neutron field of about 1.3×10^{-4} Sv/h. This corresponds to an actual absorbed dose of $\sim 10^{-5}$ Gy/h.

Our data contain various dose amounts for some types of plants. In the first batch, the plants include Arabidopsis, pine trees, and cactus. In the second batch, we again included Arabidopsis together with Azela, Euymus, and Tharuja. The plant arrangement for the first run is shown in Fig. 2 and the experimental setup for photoluminescence is shown in Fig. 3.

Fig. 2 Plant arrangement in front of neutron beam

To measure the fluorescence, we used blue laser (400 nm). Because Indium Gallium Nitride (InGaN) based laser-induced fluorescence (LIF) imaging system will image targeted fluorescence bands: 500–550 nm, 640–780 nm and near infrared. We take the fluorescence from leaves to spectrometer using optical fiber. One end of the fiber is connected to the spectrometer and the other end of the fiber was nearly touching leaves to couple fluorescent light into the fiber.

The Chlorophyll Fluorescence Emission Spectra

Under optimum condition for photosynthesis, the largest part of the light energy absorbed by the photosynthetic pigments is used for photo chemical quantum conversion to drive plant photosynthesis. Photosynthetic cells contain chlorophyll and other light-sensitive pigments that capture solar energy. In the presence of carbon dioxide, such cells are able to convert this solar energy into energy-rich organic molecules, such as glucose. These cells not only drive the global carbon cycle but also produce much of the oxygen present in atmosphere of the Earth.

Smaller portion of the absorbed light energy are remitted either as heat or as red chlorophyll fluorescence (RF). The exact amount of energy distributions is difficult to estimate and can vary per the stage of development and stress condition. The general relationship given by the following equation:

$$E(\text{energy})_{\text{absorbed}} = E_{\text{photochemistry}} + E_{\text{heat}} + E_{\text{fluorescence}} \quad (1)$$

When process of photosynthetic quantum yield is reduced due to environmental stress, the de-excitation of absorbed light energy via heat and fluorescence emission increases in contrast to heat emission, which is only detectable by special technique such as photo acoustic spectroscopy. On the other hand, chlorophyll fluorescence is easy to measure. A higher emission of RF not only occurs on the stress condition but also predarkened leaves are illuminated RF increase very rapidly to its maximum level F_m then comes to its steady-state value F_s.

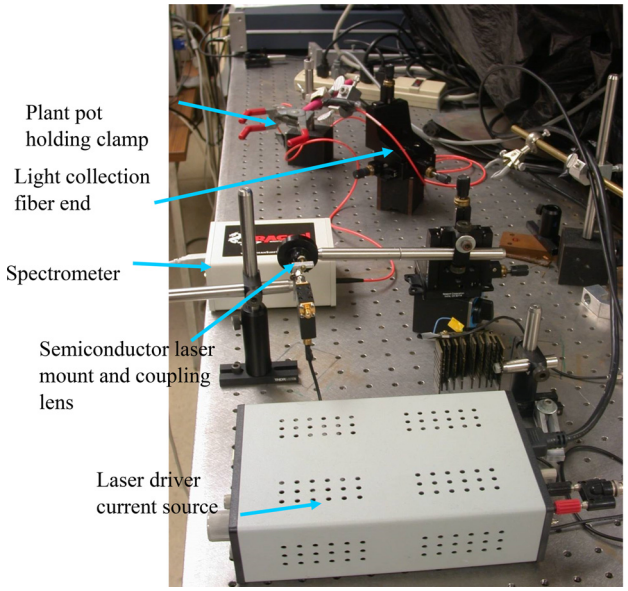

Fig. 3 Measurement setup of the plant fluorescence of the chlorophyll experimental setup

Results and Discussion

Excitation of Arabidopsis, Dwarf mango (pine), Euymus, Cactus, and Azela leaves with blue light irradiation (CW laser 400 nm) led to a fluorescence emission spectrum with two maxima of the chlorophyll fluorescence in the red spectral region near 680 nm ($\mathbf{F_{680}}$) and 735 nm ($\mathbf{F_{735}}$).

Figure 4 shows the fluorescence emission spectra of Arabidopsis and Tharuja (up and down) before radiation after radiation (left–right). It shows clearly 640–780 nm band fluorescence increase after the radiation. These are examples of typical fluorescence data we collected and some of them are collected in daily basis after the radiation. With these data sets, we can construct plots of chlorophyll $\mathbf{F_{680}}$ and $\mathbf{F_{735}}$ ratio as a function of time, which reveals the recovery time for each individual plant.

The obtained spectra showed the typical chlorophyll emission spectrum with two bands corresponding to photosystems fluorescence. The reaction centers of photosystem I (PSI) and photosystem II (PSII) in chloroplast thylakoids are the major generation site of reactive oxygen species. Photoreduction of oxygen to hydrogen peroxide (H_2O_2) called PSI. Subsequently, the primary reduced product was identified to be superoxide anion (O_2^-), and its disproportionation produces H_2O_2 and O_2. On the other hand, in PSII, oxygen of the ground (triplet) state (3 O_2) is excited to singlet state (1 O_2) by the reaction center chlorophyll of triplet excited state.

Several authors agree that at room temperature, both PSI and PSII [6–11] are responsible for the band in the far red, around 735 nm, while at 680 nm emission is only attributed to PSII. The peak fluorescence ratio $\mathbf{F_{680}/F_{735}}$ is thus connected to the balance between them and was found to vary in the presence of several factors related to plant health.

The experimental fluorescence ratios ($\mathbf{F_{680}/F_{735}}$) for samples did vary appreciably. Results for Euymus, Dwarf Mango (pine), cactus, and Azela showed a decrease in $\mathbf{F_{680}/F_{735}}$ because of facilitation of e^- transfer from PSI. On the other hand, for the Aradopsis and Tharuja showed an increase in $\mathbf{F_{680}/F_{735}}$ because either preferential damage in PSII or inhibition of e^- transfer from PSI. When time passes, the recovery process gradually brings the ratio back to its normal value.

As observed in Fig. 5, the $\mathbf{F_{680}/F_{735}}$ ratio all changed after receiving either weak or strong radiation and they all recovered to their original values but different speeds. The important information is that the recovery speed is in the range of weeks to months, not hours or years. This basically is saying that we may apply the result in couple of ways to monitor radiation. One is related to the speed. Pine tree recovery time is faster than others. Some of them will take shorter time and some may take even longer time. We may use different recovery times for event detection. For example, we may stay

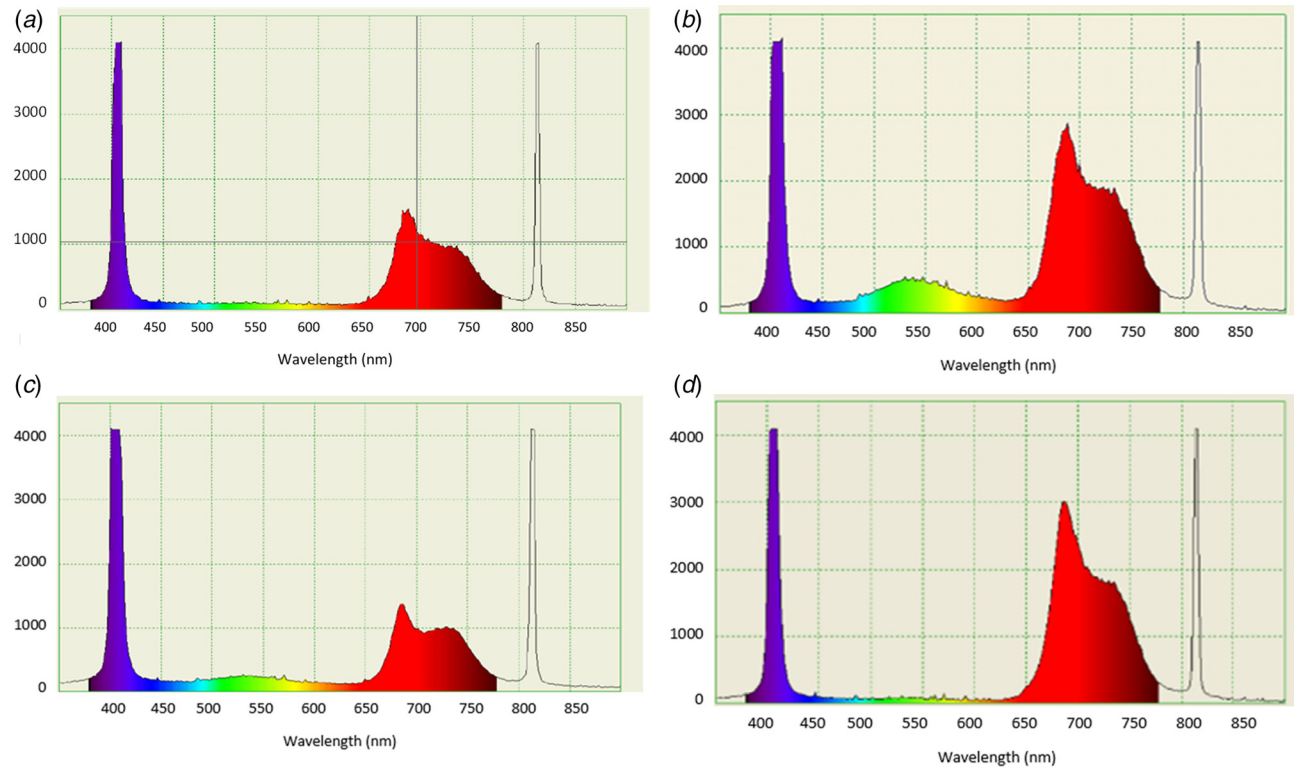

Fig. 4 Change in the shape of chlorophyll fluorescence emission spectra with radiation on leaves of Arabidopsis and Tharuja (up and down) before radiation after radiation (left–right)

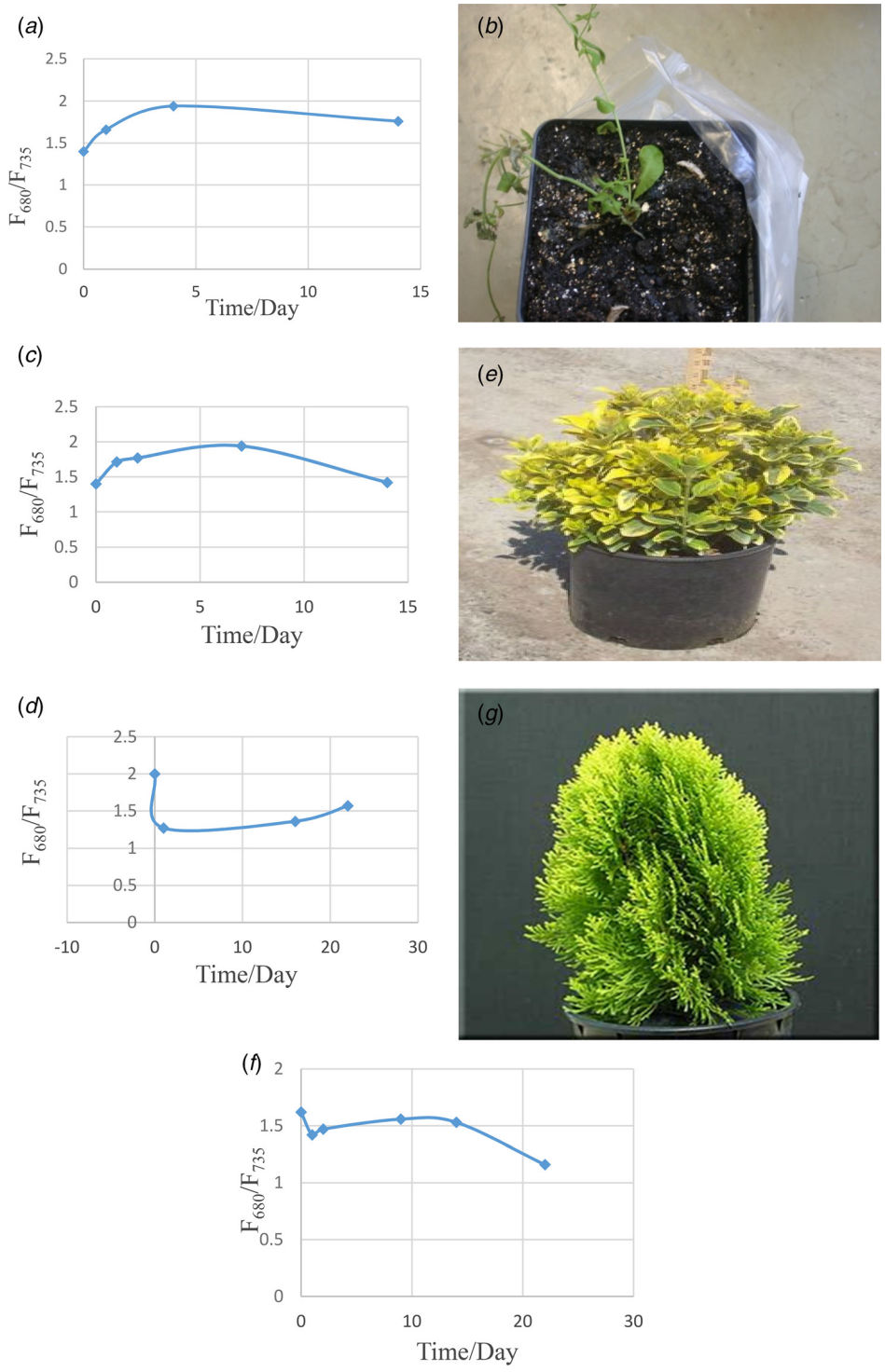

Fig. 5 Dependence of the chlorophyll fluorescence ratio F_{680}/F_{735} changing with time after plants are exposed to radiation: (*a*) Arabidopsis, (*b*) Arabidopsis, (*c*) Arabidopsis-2, (*d*) Euymus, (*e*) Euymus, (*f*) Azela, (*g*) Azela, (*h*) Tharuja, (*i*) Tharuja, (*j*) Tharuja longer rad, (*k*) pin tree-2 day rad, (*l*) pin tree-2 day rad, (*m*) pin tree-2 day rad, (*n*) pin tree-2day rad, (*o*) Dwarf mango (pine), (*p*) pin tree-1 day rad, (*q*) cactus (Echinopsis), and (*r*) cactus

in town for a few days, do measurement on different types of plants, and observe the changes, which can be helpful to project how many days earlier some nuclear activity may take place.

Here, we can also mention that people already studied Arabidopsis $\mathbf{F_{680}/F_{735}}$ ratio in cold temperatures [12]. Results were opposite to what we got for radiation effects. Short-term stress events (minutes to hours) disturb the photosynthetic performance. Long-term stress events (days to weeks) result in a decline in the chlorophyll content, which can easily be monitored via the increase in the chlorophyll fluorescence ratio $\mathbf{F_{680}/F_{735}}$. In our experiment, nuclear radiation should be considered as short-term stress.

An important point is to verify whether the observed changes in the ratio were a result from gamma radiation or due to other environmental changes. Therefore, there is a need of a reference

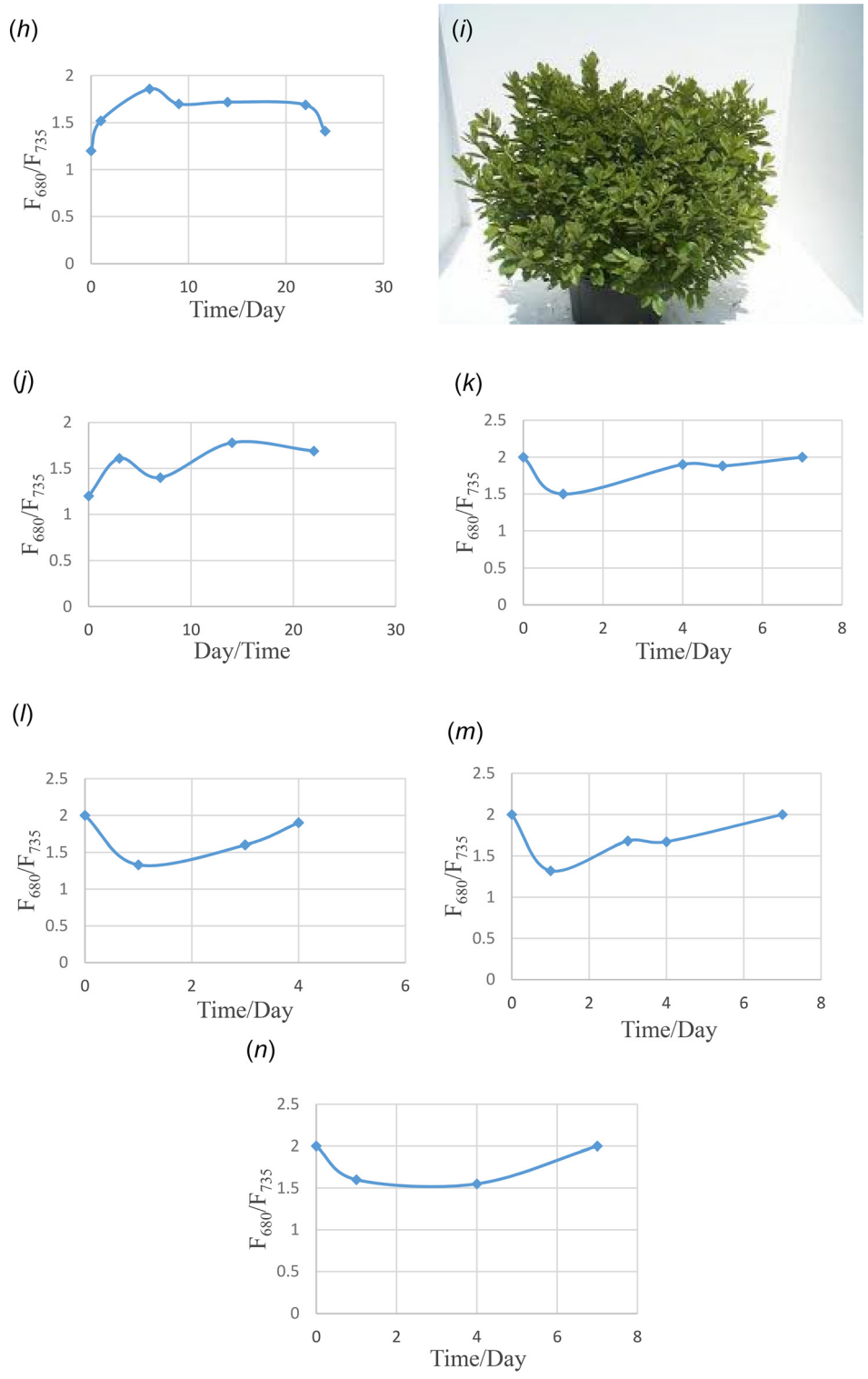

Fig. 5 (Continued)

plant that does not exhibit measurable changes in its fluorescence post gamma radiation. As such, ribwort plantain is a prime example as compared with maple tree [13–18]. This is perennial plant, which is native to Europe, Northern, and Central Asia. Long-term studies have shown that its fluorescence (both flavin/carotenoid and chlorophyll spectra) is practically not affected by the radiation. This common mode rejection and differential mode detection method shall provide us a tool for false positive alarm prevention. The maple tree can be a candidate for long-term monitoring and Ribwort Plantain can be a reference to reject common mode changes from temperature and water (drought) variations.

Probable error may come from peak value reading of spectrum graphs. The estimated reading error range is less than 2% (Table 1).

Conclusion

In this study, we have shown that all plants in room temperature used for our plants used for experiment are sensitive to nuclear radiation and they do change their normal fluorescence ratio due

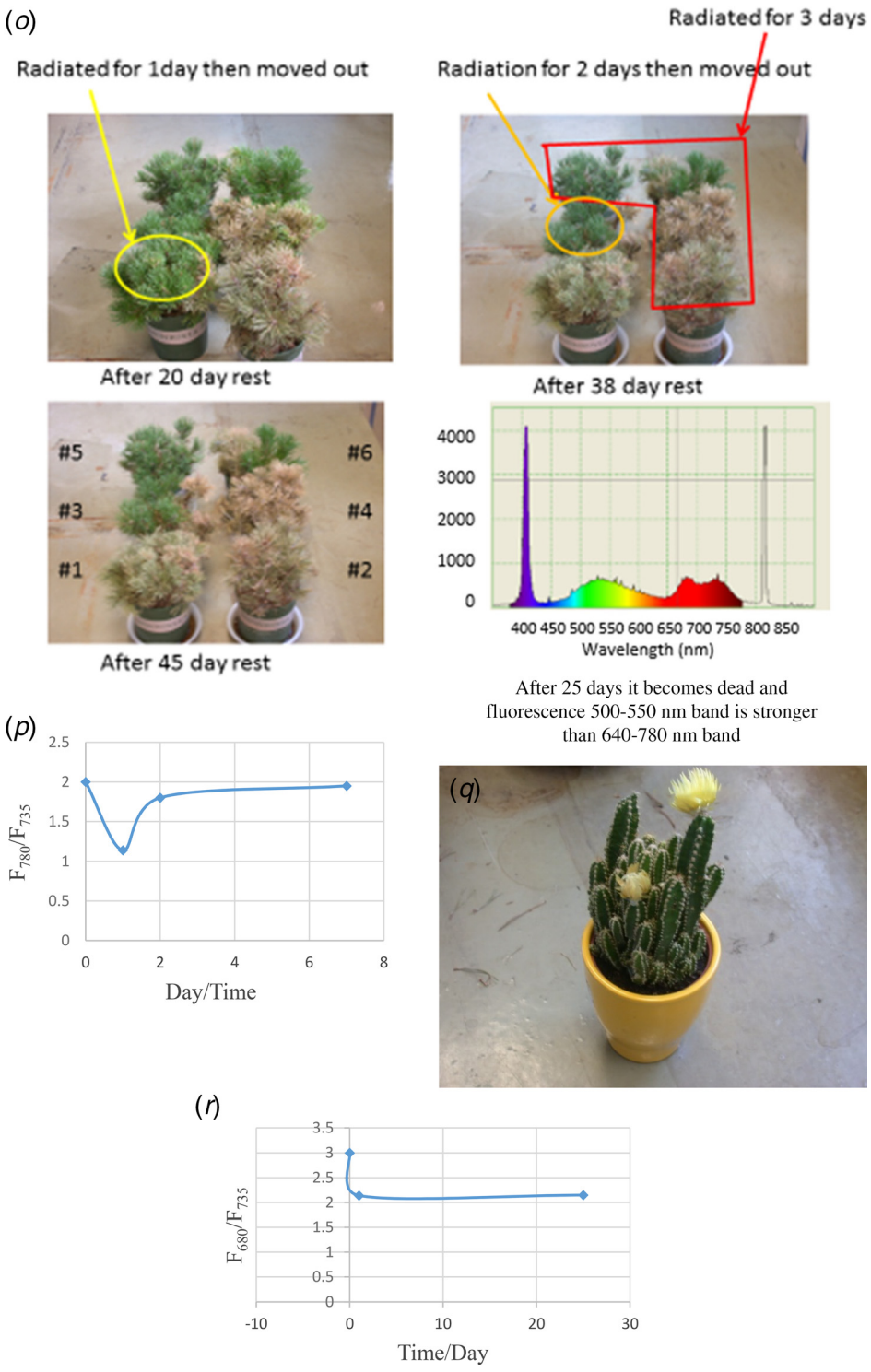

Fig. 5 (Continued)

to radiation. Some of them take longer time to recover and take less. We plan to use their characteristics to do detection and extract nuclear activity information out of measurement results.

Table 1 Measurement of error to F_{680}/F_{735} ratio

Ratio	Ratio range
F_{680}/F_{735}	±2% (no unit)

Acknowledgment

The authors would like to thank NIST Center for Neutron Research to provide the neutron beam facility.

Nomenclature

CNR = Center for Neutron Research
CW = continuous wave
F_{680} = chlorophyll fluorescence in the red spectral region near 680 nm

F_{735} = chlorophyll fluorescence in the red spectral region near 735 nm
HEN = high energy neutrons
NIST = National Institute of Standards and Technology
PSI = photosystem I
PSII = photosystem II

References

[1] Islam, M., Janssen, D., Chao, D., Gu, J., Eisen, D., and Choa, F., 2017, "Electricity Derived From Plants," J. Energy Power Eng., **11**(9), pp. 614–619.
[2] Janssen, D., Islam, M., Chao, D., Gu, J., Eisen, D., and Choa, F., 2013, "Electricity Derived From Plant Tissue," International Conference & Exhibition on Clean Energy (ICCE), Ottawa, Canada, Sept. 9–11.
[3] Iriel, A., Dundas, G., Cirelli, A., and Lagorio, M., 2015, "Effect of Arsenic on Reflectance Spectra and Chlorophyll Fluorescence of Aquatic Plants," Chemosphere, **119**, pp. 697–703.
[4] Sassolas, A., Simón, B. P., and Marty, J., 2012, "Biosensors for Pesticide Detection: New Trends," Am. J. Anal. Chem., **3**(3), pp. 210–232.
[5] Védrine, C., Leclerc, J., Durrieu, C., and Minh, C., 2003, "Optical Whole-Cell Biosensor Using Chlorella Vulgaris Designed for Monitoring Herbicides," Biosens. Bioelectron., **18**(4), pp. 457–463.
[6] Cartelat, A., Cerovic, Z., Goulas, Y., Meyer, S., Lelarge, C., Prioul, J., Barbottin, A., Jeuffroy, M., Gate, P., Agatie, G., and Moya, I., 2005, "Optically Assessed Contents of Leaf Polyphenolics and Chlorophyll as Indicators of Nitrogen Deficiency in Wheat (Triticum aestivum L.)," Field Crops Res., **91**(1), pp. 35–49.
[7] Lichtenthaler, H. K., Stober, F., and Lang, M., 1992, "The Nature of the Different Laser Induced Fluorescence Signatures of Plants," European Association of Remote Sensing Laboratories (EARSeL) Advance Remote Sensing, **1**(2), pp. 20–32.
[8] Lichtenthaler, H. K., ed., 1988, *Application of Chlorophyll Fluorescence, Kluwer Academic*, Dordrecht, The Netherlands, pp. 55–61.
[9] Lichtenthaler, H. K., and Rinderle, U., 1988, "Chlorophyll Fluorescence Spectra of Leaves as Induced by Blue Light and Red Laser Light," 4th International Colloquium on Spectral Signatures of Objects in Remote Sensing, Aussois, France, Jan. 18–22, pp. 251–254.
[10] Iriel1, A., Novo, J., Cordon, G., and Lagorio, M., 2014, "Atrazine and Methyl Viologen Effects on Chlorophyll-a Fluorescence Revisited—Implication in Photosystems Emission and Ecotoxicity Assessment," Photochem. Photobiol., **90**(1), pp. 107–112.
[11] Asada, K., 2006, "Production and Scavenging of Reactive Oxygen Species in Chloroplasts and Their Functions," Plant Physiol., **141**(2), pp. 391–396.
[12] Mishra, A., Heyer, A., and Mishra, K., 2014, "Chlorophyll Fluorescence Emission Can Screen Cold Tolerance of Cold Acclimated Arabidopsis thaliana Accessions," Plant Methods, **10**(1), p. 38.
[13] Blackburn, G. A., 1998, "Spectral Indices for Estimating Photosynthetic Pigment Concentrations: A Test Using Senescent Tree Leaves," Int. J. Remote Sensing, **19**(4), pp. 657–675.
[14] Hashimoto, A., Niwal, T., Yamamural, T., Sueharal, K., Kanou, M., Kameoka, T., Kumon, T., and Hosoi, K., 2006, "X-Ray Fluorescent and Mid-Infrared Spectroscopic Analysis of Tomato Leaves," SICE-ICASE International Joint Conference, Busan, South Korea, Oct. 18–21.
[15] Jovanic, B. R., Radenkovic, B., Despotovic-Zrakic, M., Bogdanovic, Z., and Panic, B., "Impact of Nuclear Radiation on Plants Photosynthesis and Chlorophyll Content After Bombing With U328 Enriched Bombs," Am.-Eurasian J. Sustainable Agric., **6**(1), pp. 33–43.
[16] Sanderson, B. J., 1872, "Note on the Electrical Phenomena Which Accompany Irritation of the Leaf of Dionaea Muscipula," Proc. R. Soc. Lond., **21**(139–147), pp. 495–496.
[17] The Arabidopsis Genome Initiative, 2000, "Analysis of the Genome Sequence of the Flowering Plant Arabidopsis thaliana," Nature, **408**(6814), pp. 796–815.
[18] Chappelle, E. W., Kim, M. S., and McMurtrey, J. E., 1992, "Ratio Analysis of Reflectance Spectra (RARS): an Algorithm for the Remote Estimation of the Concentrations of Chlorophyll a, Chlorophyll b, and Carotenoids in Soybean Leaves," Remote Sensing Environ., **39**(3), pp. 239–247.